

### 3.3 Passive Pre-Chamber Spark Plug for Future Gasoline Combustion Systems with Direct Injection

---

Matthias Blankmeister, Muhammed Alp, Eriko Shimizu

#### Abstract

The challenge of using a pre-chamber spark plug for future gasoline combustion processes with direct injection is, on the one hand, to realize an ignitable mixture in the pre-chamber at low load and speed. On the other hand, at high speed and high load, keeping component temperatures have to be kept low in order to prevent irregular combustions (pre-ignition, glow ignition).

With increasing requirements regarding fuel consumption and emissions, the challenges to modern combustion strategies are growing steadily. Measures to further increase the efficiency of the combustion engine are required for this purpose. There are different approaches to increase efficiency. These include increasing the compression ratio and diluting the air-fuel mixture. The latter can be generally classified into two broad categories: Dilution with air and dilution with residual gas. In both cases, it turns out that the highest possible dilution is to be preferred with respect to combustion efficiency. Increasing dilution, however, leads in both cases to a deterioration in flammability and a decrease in the flame velocity of combustion. In the resulting requirements for the ignition system, the passive pre-chamber spark plug is an interesting alternative to the conventional spark plug. Due to its functional principle, it can simultaneously improve the ignition and shorten the burn duration. In the present work, the focus is on the behavior of the pre-chamber spark plug while diluting the cylinder charge with air.

A particular challenge for the passive pre-chamber spark plug is to safely ignite the mixture at idling and in the low to medium part load with a correspondingly high internal residual gas content. Dilution of the cylinder charge with air also complicates the possibility to have a good air-fuel mixture within the pre-chamber. In order to ensure a reliably ignitable mixture in the pre-chamber even under these boundary conditions, it is necessary to design a suitable pre-chamber geometry in conjunction with the direct injection.

This work describes the behavior of different passive pre-chamber spark plugs when using lean mixtures at low and medium part load with CFD simulation. Criteria such as residual gas content and air-fuel ratio at start of ignition at the ignition point as well as other flow parameters such as temperature, velocity and turbulent kinetic energy are examined in detail. The effect of the torch coming out of the pre-chamber is finally assessed by combustion simulation.

## Kurzfassung

Die Herausforderung bei dem Einsatz einer Vorkammerzündkerze für zukünftige Otto-Brennverfahren mit Direkteinspritzung ist es, zum einen bei niedriger Last und Drehzahl ein zündfähiges Gemisch in der Vorkammer zu realisieren. Zum anderen bei hoher Drehzahl und hoher Last die Bauteiltemperaturen niedrig zu halten, um eine irreguläre Verbrennung (Vorentflammung, Glühzündung) zu verhindern.

Mit stetig steigenden Anforderungen an den PKW-Motor hinsichtlich Verbrauch und Emissionen, wachsen auch die Herausforderungen an die modernen Verbrennungsstrategien. Maßnahmen zur weiteren Wirkungsgradsteigerung der Verbrennungskraftmaschine sind hierzu erforderlich. Es existieren verschiedene Ansätze zur Erhöhung der Effizienz. Hierzu zählen unter anderen die Erhöhung des Verdichtungsverhältnisses und die Verdünnung des Luft-Kraftstoff-Gemisches. Letzteres lässt sich im Allgemeinen in zwei Kategorien unterteilen: Die Verdünnung mit Luft und die Verdünnung mit Restgas. In beiden Fällen zeigt sich, dass eine möglichst hohe Verdünnung zielführend für einen hohen thermischen Wirkungsgrad ist. Steigende Verdünnung führt jedoch in beiden Fällen zur Verschlechterung der Entflammbarkeit und zur Abnahme der Brenngeschwindigkeit. Bei den hierdurch entstehenden Anforderungen an das Zündsystem stellt die passive Vorkammerkerze eine interessante Alternative zur Standard Hakenkerze dar. Aufgrund ihres Funktionsprinzips kann sie gleichzeitig zur Verbesserung der Entflammung und der Beschleunigung des Durchbrandes führen. In der vorliegenden Arbeit wurde der Fokus auf das Verhalten der Vorkammer bei Verdünnung der Zylinderladung mit Luft untersucht.

Eine besondere Herausforderung für die passive Vorkammerkerze besteht darin, das Gemisch bei Leerlauf und in der unteren bis mittleren Teillast bei entsprechend hohem, internen Restgasgehalt, sicher zu entflammen. Eine Verdünnung der Zylinderladung mit Luft erschwert ebenfalls die Darstellung eines gut brennbaren Luft-Kraftstoff-Gemisches innerhalb der Vorkammer. Damit auch unter diesen Randbedingungen das Gemisch in der Vorkammer sicher zündfähig ist, gilt es eine geeignete Vorkammergeometrie in Verbindung mit der Direkteinspritzung zu gestalten.

Im Beitrag wird das Verhalten unterschiedlicher passiver Vorkammerkerzen beim Einsatz von mageren Gemischen bei niedriger und mittlerer Teillast mittels CFD Simulation beschrieben. Kriterien wie Restgasgehalt und Lambda zum Zündzeitpunkt am Zündort sowie weitere Strömungsgrößen wie Temperatur, Geschwindigkeit und turbulente kinetische Energie werden detailliert untersucht. Die Wirkung der Fackelaustrittsbohrungen wird anschließend mittels Verbrennungssimulation bewertet.

# 1 Introduction

The advantages of pre-chamber ignition systems for spark ignited engine concepts are well known. The main differences to a conventional spark plug ignition system are illustrated in Figure 1.

The passive pre-chamber spark plugs are standard in many stationary gas engines, mainly for block heating power plants. In such applications lean limit is extended up to  $\lambda = 1.8$  ( $\lambda$  corresponds to the reciprocal value of the equivalence ratio  $\Phi$ ) due to higher combustion stability and faster combustion compared to conventional spark plugs. These latest developments were referring to the Clean Air Act (TA Luft) [1] and power ratings of 0.8 to 2.5 MW, suitable for use with natural and other special gases [2].

Another area in which the passive pre-chamber spark plug is used is motorsports. Similar to stationary gas engines, the main focus in motorsports is the operation of the engine at high load. The functional design on a quasi-singular operating point is readily implementable, and therefore the use of the pre-chamber spark plug in these two areas is now state of the art.

The use of the passive pre-chamber spark plug in a mobile application, e.g. a passenger car is currently not possible. The reason for this is the operation from cold start, idle over part load to full load. All operating points must be ensured and up to now this has not been proven with a single pre-chamber spark plug. At the two extreme operating points, low part load (idle) and full load, there are different challenges towards the pre-chamber spark plug. At low load, despite low pressure sufficient fuel in the pre-chamber is required to ignite the mixture reliably. At high speed and high load, the challenge for the pre-chamber spark plug is to keep component temperatures low to prevent irregular combustion (pre-ignition, glow ignition).

This article focusses on the first part, the analysis of the behavior of different passive pre-chamber spark plug when using lean mixtures at low and medium part load by means of CFD simulation with and without combustion and also at the test bench.

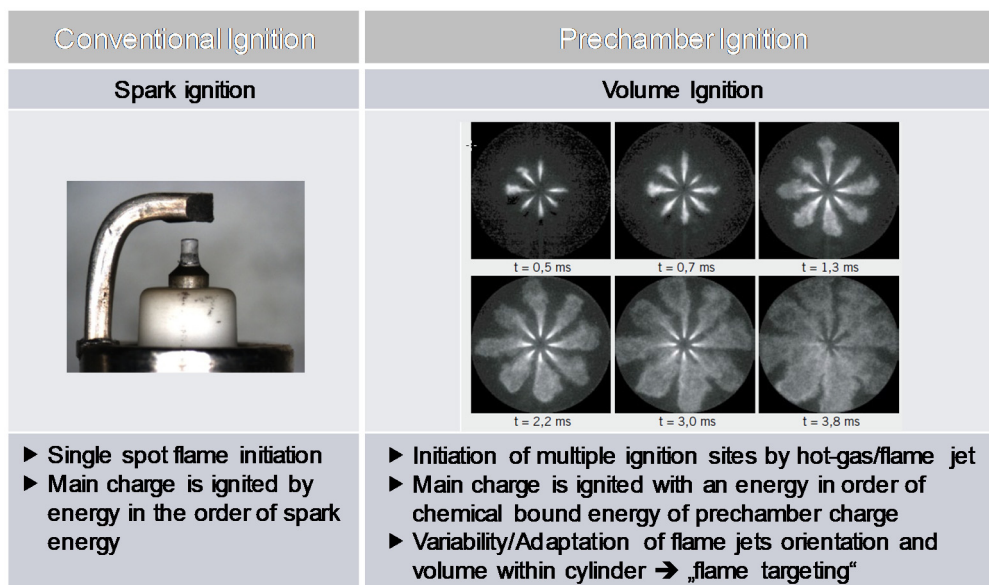


Figure 1: Comparison of conventional spark ignition and pre-chamber ignition with picture of OH-Chemiluminescence measurement combustion of a pre-chamber ignition system [3]

## 2 Design

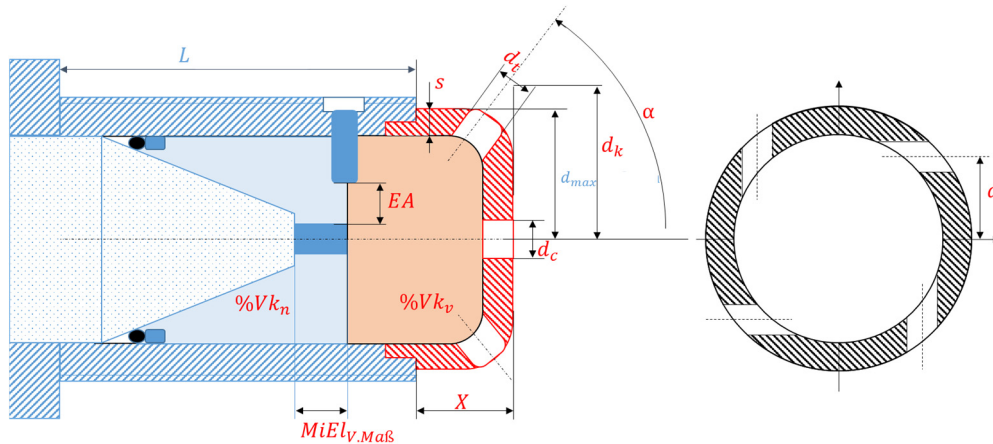


Figure 2: Schematic drawing and example of a pre-chamber spark plug

There are many different approaches belonging to the design of a passive pre-chamber spark plug. The idea of the Bosch approach was to accomplish a design suitable as a plug-and-play solution for an existing cylinder head with a conventional spark plug design. This approach is shown in Figure 2. The design philosophy has some characteristic elements. Besides the insulator, center electrode and the housing it includes a ground electrode with a special implementation and the pre-chamber cap mounted directly onto the housing of the pre-chamber. As can be seen, there are many geometrical parameters that theoretically can be varied.

To reduce the amount of variants for the planned CFD simulation study to a convenient level, two things were done. Firstly, it was decided only on a certain set of parameters to be varied. Secondly, the number of increments in each parameter dimension was reduced by using a simple two step approach based on the idea of a reference geometry. The design of the reference geometry was derived from empirical values and values from literature, such as for example pre-chamber volume, hole diameters and hole angles.

Figure 3 shows the seven parameters, which were chosen to be varied, as shown in the left hand box. All parameter variations which led to the other pre-chamber geometries to be investigated were derived on bases of the aforementioned two step approach.

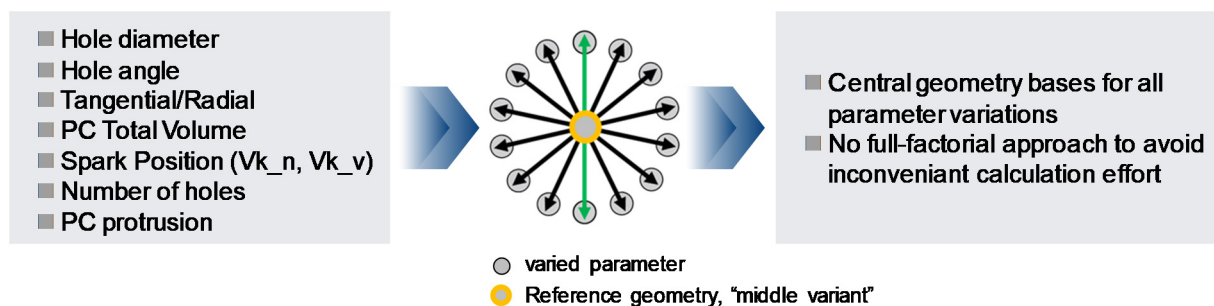


Figure 3: Investigation approach for CFD investigations

This means each change was made based on the reference geometry in such a way that a change to a parameter's value was made into one direction and another to the opposite direction referring to the mentioned reference geometry. For example the hole

diameter was increased by 0.3 mm for one variant and decreased by 0.3 mm for another variant. This manner of variations helps understand sensitivities of system on a basic level with reasonable effort. The symbol in the middle of Figure 3 is representing this scheme. Eventually this approach leads to a non full-factorial approach, reducing the simulation effort significantly.

An overview of the designs which were derived based on the described approach can be found in Figure 4. The illustrated pictures of the different variants represent the inner gas volume of the pre-chamber spark plug including the holes connecting the pre-chamber volume to the main chamber volume. In other words, these are the fluid domains used by the CFD model for the simulation.

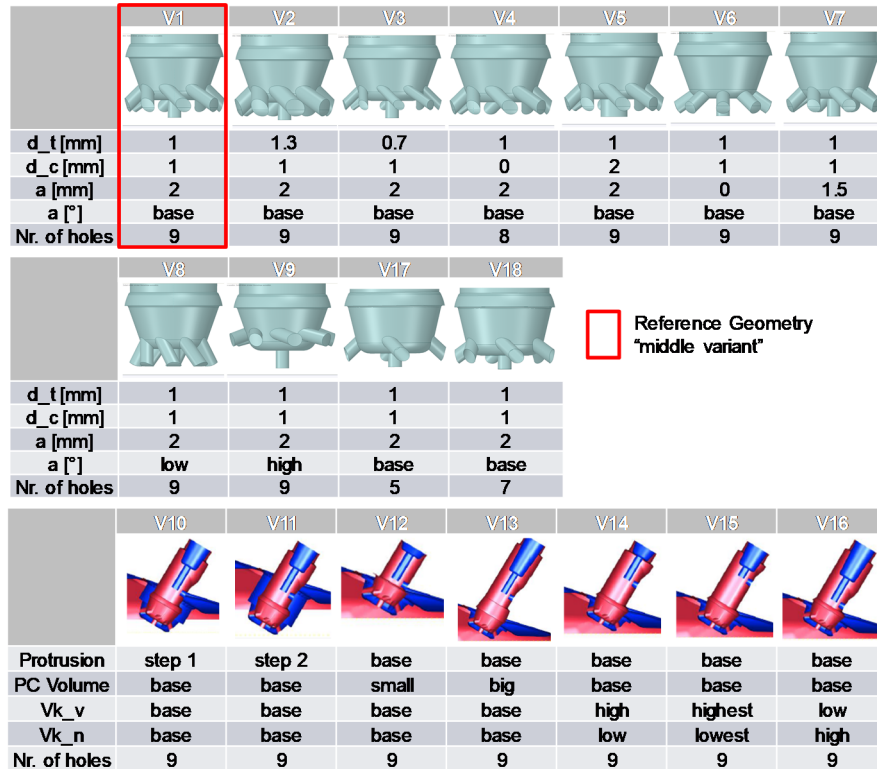


Figure 4: Overview investigated pre-chamber Variants

Variants V10 to V16 have the same hole designs (hole diameter etc.). Changes are made regarding V1 so that parameters can be clustered into a pair of geometries, for which a certain geometrical parameter was changed.

### 3 CFD Simulation

To establish a better understanding of the dominating physics within the pre-chamber spark plug 3D CFD simulations were conducted.

In this study the different pre-chamber variants were compared amongst each other based on residual gas mass fraction, t<sub>ke</sub> and equivalence ratio at ignition timing. These CFD results were then used to derive a ranking of pre-chamber spark plugs and consequently to help decide for samples to be used on the engine test-bench.

Due to the importance of the gas exchange for the evaluation of the pre-chamber scavenging the simulations comprise the full 720 °CA cycle.

The residual gas mass fraction will be denoted as “EGR” in this paper, even though this word is usually used for external gas recirculation.

### 3.1 CFD Model Setup

Simulations were done using an in-cylinder geometry, including intake and export ports, a DI injector and the spark plug. The illustration Figure 5 shows the CFD model with the base pre-chamber variant integrated.

All 3D CFD calculations were conducted with the commercial Software AVL Fire, using the RANS approach. Furthermore, the k-zeta-f turbulence model was used. For the liquid phase n-heptane was used as reference species. For the spray the wave break-up model was used and the spray temperature was set to 343.15 K. Constant wall temperatures were used for all wall boundaries.

The geometrical model for the in-cylinder simulation is based on an engine combustion chamber containing complete intake and exhaust ports and a central DI injector.

As depicted in Table 1, two operation points were chosen to be investigated via the CFD simulation. The nomenclature b. IDTC means “before ignition top dead center”.

Table 1: Simulated operation points

Operation Point	Engine Speed [rpm]	Imep [bar]	SOI [°CA b. ITDC]	$\lambda = 1/\Phi$ [-]
OP1	1500	3	330	~ 1.6
OP2	2000	8	330	~ 1.5

OP1 with low engine speed and low load was chosen to address a pre-chamber operation at relatively high residual gas mass level, small in-cylinder charge and low charge motion level. OP2 represents higher part-load with mid-range engine speeds, which was intensively investigated and optimized on preliminary studies on homogeneous lean combustion.

In Figure 5 the geometrical setup of the pre-chamber within the combustion chamber is illustrated. In this study predominantly two volumes have been used for the CFD evaluation: the total pre-chamber volume and the main chamber. As also can be seen in the illustration, the chosen spray pattern (blue) of the multi-hole injector does not involve any beam which directly points to the pre-chamber spark plug.

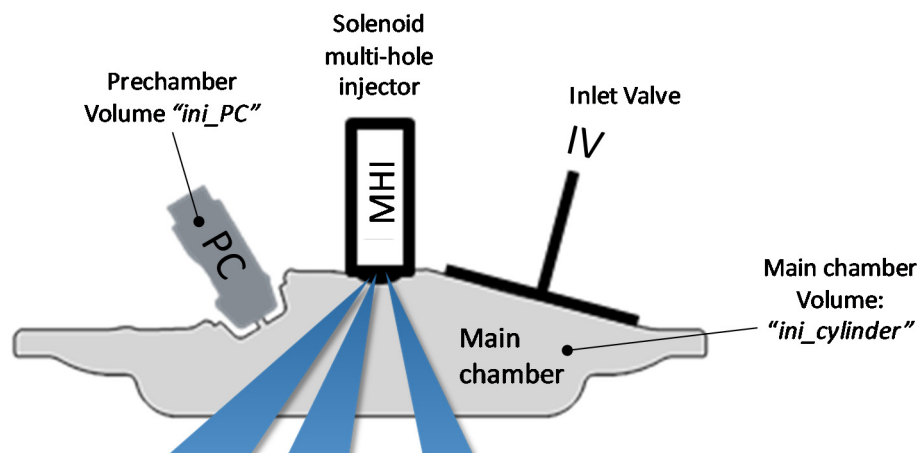


Figure 5: CFD in-cylinder model cut plane

## 3.2 Results

The results of the gas exchange and mixture preparation simulations will be illustrated and explained in two steps: first a qualitative analysis of the flow field and mixture condition based on 3D and 2D evaluation will be shown. Secondly the results will be quantified in chosen volumes by integrating the values in all of its cells and then averaging them, so that the development of the mixture within the pre-chamber over crank angle can be analysed.

Eventually the condition of the mixture at ignition timing will be analysed and representative values will be plotted against each other to evaluate if and what kind of correlations can be found.

### 3.2.1 Comparison of Operation Points

In Figure 6 residual gas mass fraction (“EGR”), lambda  $\lambda$  and the turbulent kinetic energy (“tke”) are illustrated for operation points OP1 and OP2. The blue coloured circles symbolize the mean value over all pre-chamber variants simulations at 695 °CA (25 °CA BITDC) for the ini\_PC volume for OP1 and respectively OP2. The grey coloured circles show the mean value of all simulations for the ini\_cylinder volume.

The ignition timing was assumed to be within the relevant region at the beginning of the CFD study.

Comparing the two evaluated volumes, the pre-chamber volume shows higher EGR values, higher lambda values and lower tke values compared to the main chamber, as can be expected. It is worth noting, that the discrepancy for the lambda value between pre-chamber volume and main chamber volume has the tendency to decrease for higher load and engine speed operation points. In other words, a richer lambda can be reached within pre-chamber volume for increasing load and engine speed at the same main chamber lambda value.

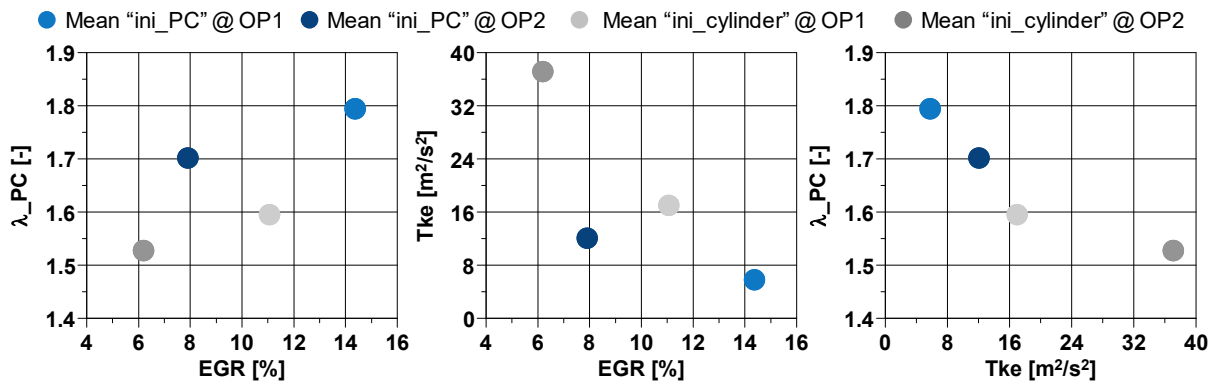


Figure 6: Mean values of egr, lambda, tke at OP1 & OP2

### 3.2.2 Crank Angle Based Analysis of EGR, Tke & Equivalence Ratio

In this section a more detailed analysis of the EGR, tke and lambda within the pre-chamber will be discussed. In the following illustrations the dotted black lines describe the integrated mean values for the main chamber volume (“ini\_cylinder”), while the grey solid lines denote the behaviour within the pre-chamber volumes (“ini\_PC”). The vertical blue lines represent inlet valve opening and respectively closing. The orange vertical line represents fuel injection timing. Furthermore contour plots of variant V1 are used to indicate the spatial distribution of the values at 695 °CA (25 °CA BITDC).

For easy comparison the same timing was used to evaluate the pre-chamber variants at OP1.

In Figure 7 the trends for EGR over crank angle degree for all pre-chamber variants are illustrated. For almost all variants the EGR level in the pre-chamber volume is higher than the main chamber level independent from the operation point. For both OP the highest EGR level can be found for the variant V3, where the total flow cross section is the smallest which describes the sum of each hole cross section area. The variant V12, which has the smallest total pre-chamber volume on the other hand has the lowest EGR level in both operation point cases. In fact, for the OP2 it even reaches a slightly lower EGR level than the main chamber charge already at the end of the intake stroke. Obviously, total residual gas mass at the beginning of scavenging is less for variant V12 than all the other variants with bigger volume.

The EGR distribution plots show a tendency of EGR to accumulate around the pre-chamber axis. This is due to the swirl induced by the tangentially arranged radial bores.

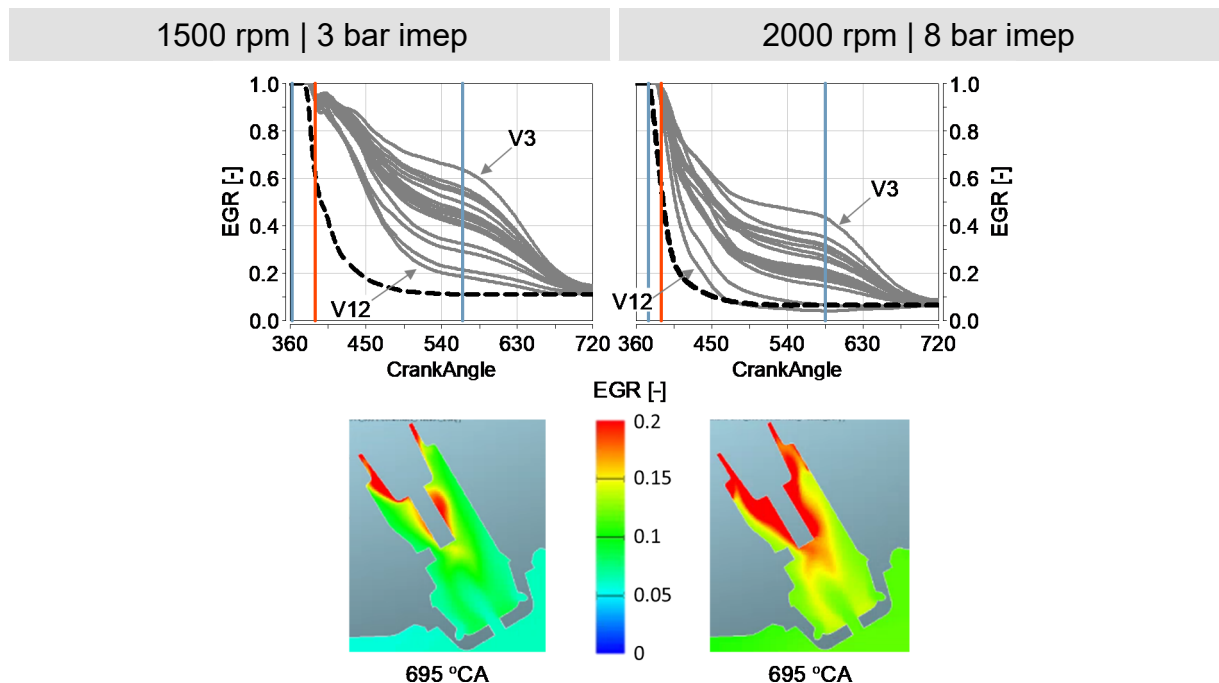


Figure 7: Comparison pre-chamber variants, EGR trends and distribution

The main chamber EGR level after inlet valve closing determines the minimum EGR level within the pre-chamber volume which can only be reached asymptotically. Much of the change in EGR is already happening within gas exchange phase. During compression EGR values further decrease rapidly. The upward movement of the piston causes a pressure difference between the main chamber and the pre-chamber volume. This in consequence feeds the pre-chamber volume with the main chamber air-fuel mixture with its main chamber EGR level.

On basis of this observation one can conclude that, without the consideration of the scavenging in the gas exchange phase, the mean EGR level of the total pre-chamber volume at the end of compression will almost exclusively depend on the ratio between pre-chamber volume and main chamber volume. Additionally, it can be concluded, that the actual residual gas mass within the pre-chamber is determined by the gas exchange phase from inlet valve opening up to the point when main chamber pressure

exceeds the pressure in the pre-chamber volume. After this EGR level only changes by displacing the resident residual gas mass of the pre-chamber volume by the main chamber mixture with lower EGR level.

Analysing the tke levels and trends illustrated in Figure 8 the results show, that the tke values reached within the pre-chamber variants are always lower than within the main chamber. Furthermore it can be observed that the positions of tke peaks close to ITDC are very similar comparing between main chamber and pre-chamber volumes.

The variant V3 reaches for both variants high tke levels.

Contrary to V3 the variant V12 shows the lowest tke values. This can be explained by the fact that when the piston moves up and the condition  $\Delta p = p_{pc} - p_{mc} < 0$  is met, the mass flow into the pre-chamber volume to equalize the pressure difference is the lowest compared to the other variants.

The contour plots show that tke is mainly generated at the holes. The increased load and engine speed at OP2 push up regions of high tke towards the spark position.

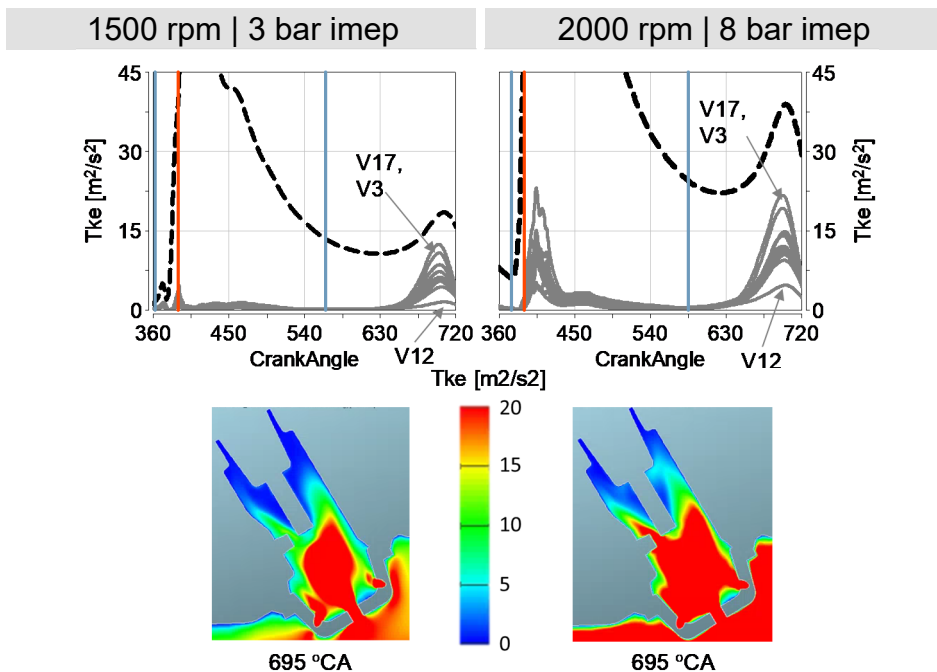


Figure 8: Comparison pre-chamber variants, Tke trends and distribution

Another important aspect of the passive pre-chamber spark plug is the equivalence ratio  $\Phi$  within the pre-chamber, which is illustrated in Figure 9.

In both operation point cases, the main chamber mixture is already settled to a constant value at bottom dead center (540 °CA), which it keeps unchanged until the end of compression. However, in the pre-chamber volumes  $\Phi$  change significantly after inlet valve closing.

In compression phase, mixture with a  $\Phi$  ratio of the main chamber level is pushed into the pre-chamber volume, causing an asymptotic approximation to main chamber level, quite similarly as for the behaviour of the EGR values shown before.

Especially for OP1 the pre-chamber variants show a significant increase in  $\Phi$  within the gas exchange phase. This phenomenon in principle can also be seen for OP2 but in a much more moderate level.

The low load case OP1 will have less fuel injected leading to lower penetration of the fuel into the main chamber. This in return leads to a rich zone closer to the holes during scavenging phase than compared to OP2.

The highest  $\Phi$  values at ignition relevant timings is reached by the variant V6 for OP1 and Variant V3 for OP2.

For OP1 the pre-chamber volume can reach a value of  $\Phi$  very close to that in the main chamber volume. For OP2 this is not the case.

The contour plots, showing an accumulation of leaner regions around the pre-chamber axis, representing a very similar structure like the EGR distributions.

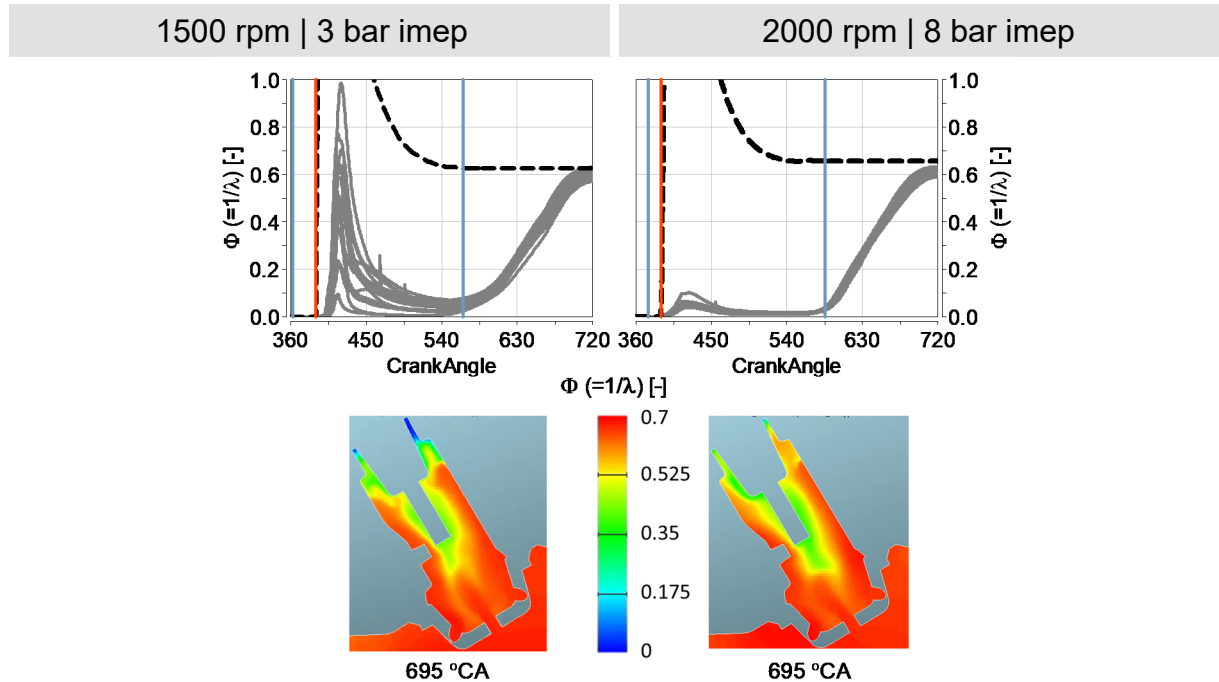


Figure 9: Comparison pre-chamber variants, A/F trends and distribution

As described before there are similarities to the EGR behaviour. However, a big difference is the  $\Phi$  distribution within the main chamber. The inhomogeneities with respect to  $\Phi$  will be much higher than for EGR. Therefore timing of the injection as well as the geometries will have an influence on the trend within the pre-chamber volume.

### 3.2.3 Scavenging Mechanism & Flow Pattern

The mechanism of scavenging will be illustrated and explained by Figure 10. The A-A cut section plane is used to show the mass exchange, between main chamber and pre-chamber volume, in which the uniform length and colour velocity vectors are used to demonstrate the direction of flow. The illustrated results belong to the case OP2, pre-chamber variant V1. The colours illustrate the distribution of EGR. The scaling of EGR is used only up to 0.5 so differences get more distinguishable.

On picture (a) of Figure 10, a few degrees after gas exchange top dead centre one can clearly see that mass is only transferred from pre-chamber volume to the main chamber volume, indicated by the vectors in each hole pointing outwards. In this case (OP2) inlet valves open around 375 °CA. Up to that time, gas with EGR = 1 is leaving the pre-chamber volume. That means residual gas mass is decreasing, but the fraction of residual gas within the pre-chamber stays constant, because gas is only flowing out of

the pre-chamber, without any gas with EGR level lower than 1 entering the pre-chamber. Therefore the level within the pre-chamber volume is not decreasing.

This is also shown by the EGR curves in Figure 7 for OP2, which show that EGR level is left at  $EGR = 1$  until inlet valves open. For OP1 it can be observed that the decrease in EGR level happens later than inlet valve opening timing. This is due to the fact, that in contrast to OP2, OP1 represents a throttled operation point. At inlet valve opening timing the inlet ports still feature a lower pressure than the cylinder.

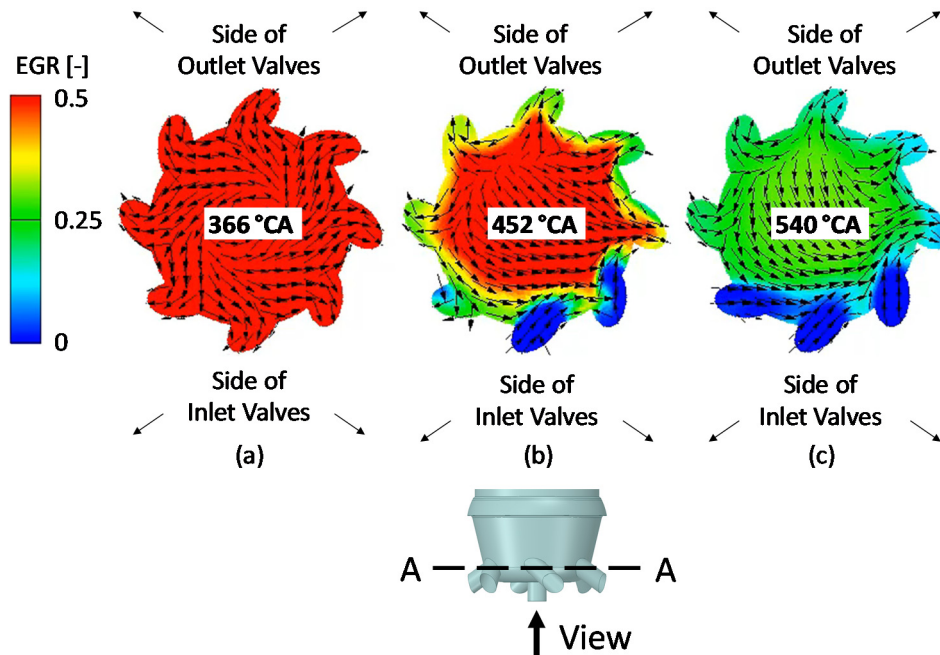


Figure 10: Scavenging mechanism (residual gas mass fraction EGR)

In picture (b) it two of the 8 shown holes implicate a massflow from the main chamber to the pre-chamber, while the rest of the holes show an outward flow. The entering gas seems to have an EGR level as low as around 0 indicating, that the pre-chamber volume is fed with fresh air. This picture represents a flow through the pre-chamber volume, which in consequence decreases the EGR level.

When the flow from the intake ports enter the main chamber a portion of it stagnates at the side of the pre-chamber spark plug cap, which is oriented towards the inlet valves generating a small over-pressure compared to the back side of the cap, which is oriented to the outlet valves. Even slow pressure differences as low as 5 mbar are sufficient to establish the scavenging process. The swirl created by the tangential inclination of the holes has an upward movement within the pre-chamber volume, which is caused by the vertical inclination denoted by the  $\alpha$ -angle in Figure 4. This leads to the scavenging of also the upper parts of the pre-chamber volume.

The swirl induces a flow through its core from top down. The described phenomenon & flow pattern is true for both EGR and  $\Phi$ . This can be seen in Figure 11 showing a typical structure of distribution for  $\Phi$  for all variants with tangentially oriented radial holes. The distribution for EGR has already been shown in Figure 7.

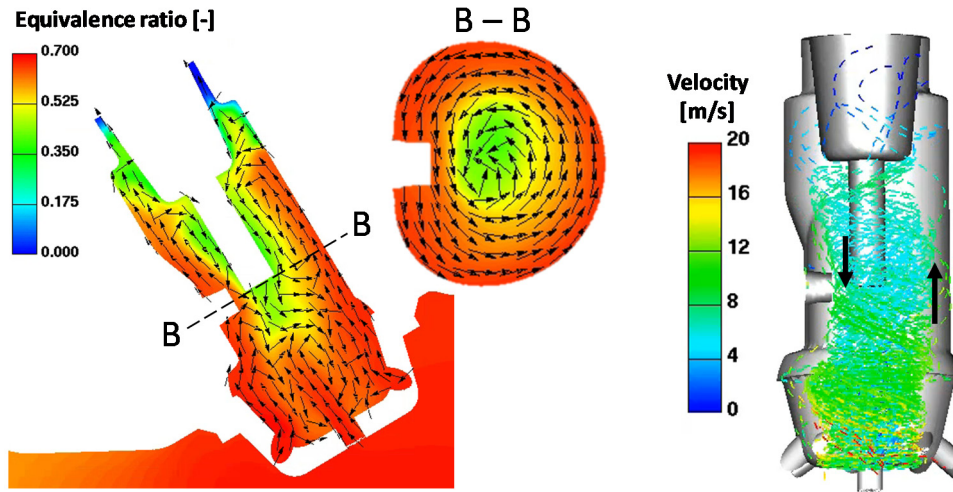


Figure 11: Typical flow pattern including EGR distribution at 25 °CA bITDC at OP1

### 3.2.4 Correlations

In the following section correlations between the different pre-chamber geometries and the CFD results at 695 °CA will be made, to evaluate the pre-chamber variants with respect to ignition condition. In Figure 12 pre-chamber variants V1, V3 and V12 were chosen, to show the correlations between EGR, tke and some of the geometrical parameters. In these plots a tradeoff between scavenging and tke is depicted.

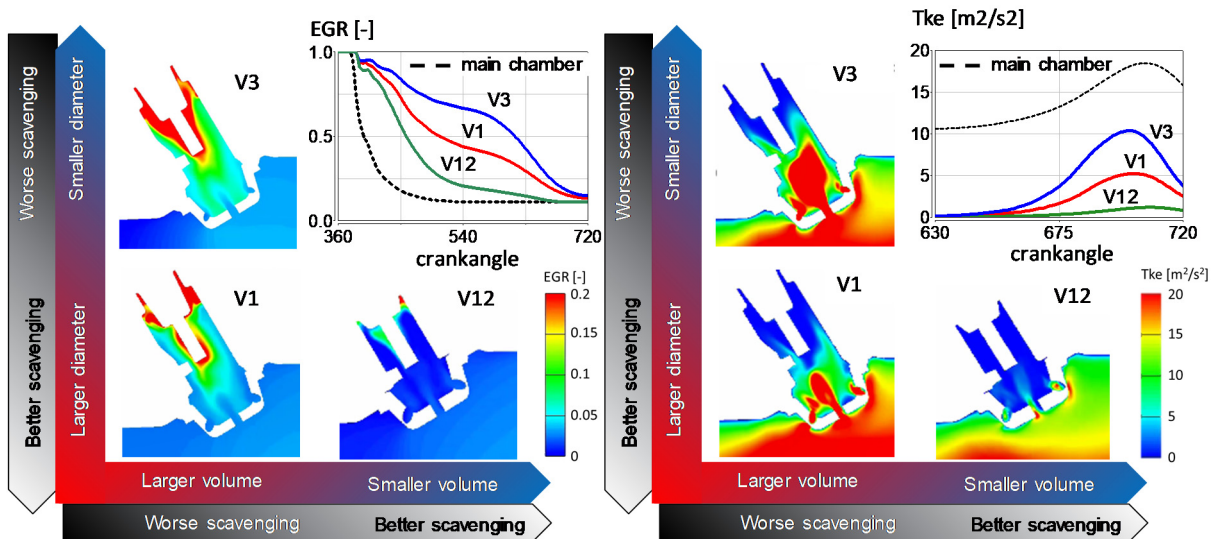


Figure 12: Correlations of geometry, EGR and tke at OP2

One can see that decreasing the volume or increasing the hole diameters have the same effect on EGR and tke. But while decreasing the volume or increasing the hole diameters help increase the scavenging quality, it deteriorates the tke.

The change in hole diameters will change the total flow cross section A. The ratio between A and the pre-chamber volume V is called the A/V ratio, which is widely known to be a value for the characterization of pre-chamber geometries.

Additionally to the above mentioned correlations Figure 13 illustrates  $\lambda$  ( $=1/\Phi$ ) and the CFD results are also plotted against the geometrical characteristic A/V. The values are representing the conditions at 25 °CA bITDC (695 °CA). Here the circles in

light blue represent the operation point OP1 and the dark blue operation point OP2. The numbers in the circles represent the pre-chamber variant.

It can be seen that in terms of lambda OP1 has a wider range than OP2 and some variants have a very lean mixture condition, for example V12 with around 1.95. This is very critical because at low loads combustion is per se more challenging, but shows at the same time that much can be done by geometrical variation only.

Analysing the variants which had a good scavenging quality, namely V12 and V2, the results indicate, that best scavenging behaviour is not correlating with highest enrichment within pre-chamber.

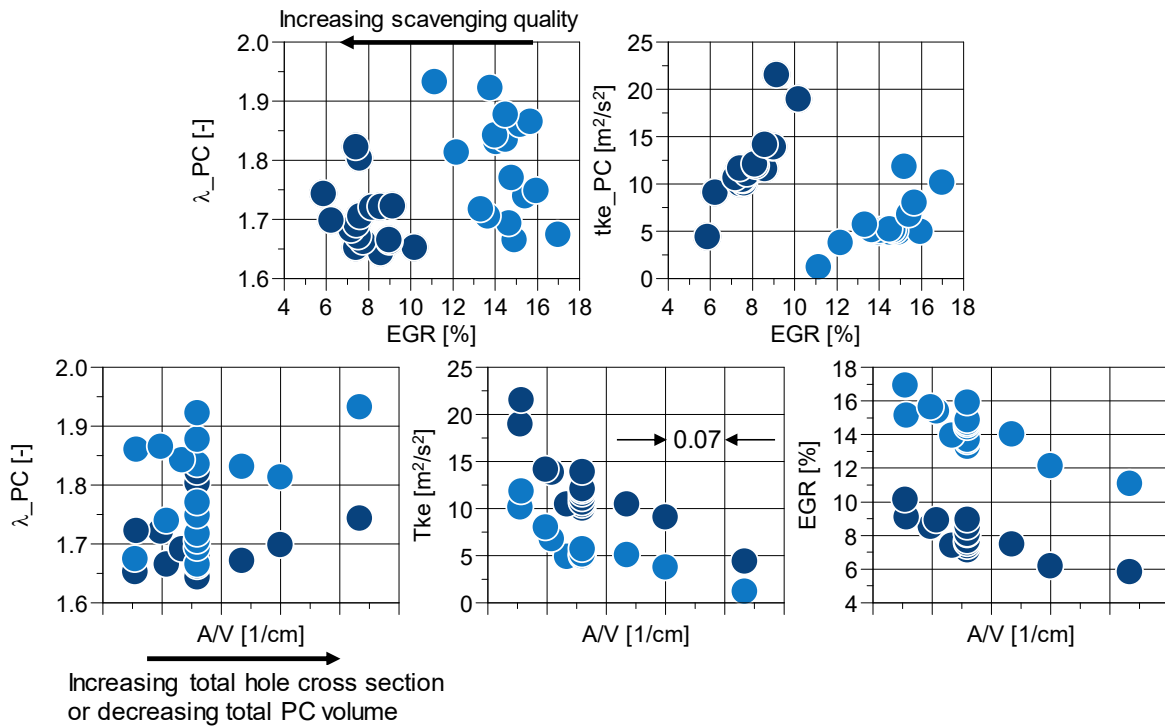


Figure 13: Correlations between geometries and several CFD results

Looking at the plots of A/V ratio, another major deduction of the results is that at the same A/V there is a very broad range of lambda in the pre-chamber achievable. This means, only by changing the orientation and angles of the pre-chamber geometries one can obtain very different results with respect to enrichment of the pre-chamber volume. The aforementioned influence of hole diameters and volume on tke and EGR can be observed in the A/V plots.

This A/V ratio is not only relating the geometrical design of the pre-chamber to EGR, tke, lambda at ignition timing, but it will particularly have an influence on the combustion. While the volume represents the magnitude of mixture energy stored into the pre-chamber and theoretically accessible for combustion, the flow cross section will be key to the magnitude the pressure of the pre-chamber will exceed the pressure in the main-chamber. Low A/V will lead to a higher pressure difference between pre-chamber and main chamber ( $\Delta p$ ) and therefore further penetration of the jets into main chamber than a variant with higher A/V ratio. This jets can be either hot gases without a flame transported into main chamber, involving intermediate species (radicals) and products of combustion or flame jets, which involve an active flame within [1],[4].

### 3.2.5 CFD Ranking

Based on the results shown in Figure 13, a scoring model was used to rank the different pre-chamber variants among each other. This ranking was used to decide, which variants will be used for engine test-bench. Different weightings for egr, lambda and tke were used for the scoring. After evaluating scorings for each considered weighting scenario in a crank angle region, which is relevant with respect to ignition timing four pre-chamber variants were chosen as illustrated in Figure 14.

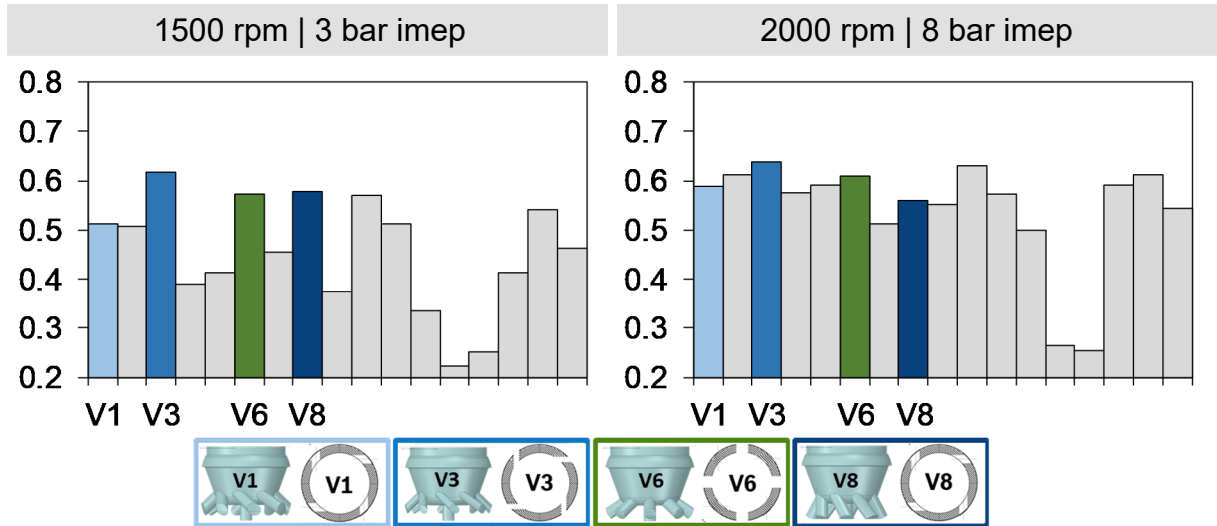


Figure 14: Scoring of all pre-chamber variants

The values on the y-axis represent the score with a minimum of 0 and a maximum of 1 based on the principle of the scoring model. Beneath the scoring diagrams the variants which were chosen for the engine test-bench are shown, which include variation of orientation of the radial holes on the horizontal plane (V6), change of the vertical inclination of the holes (V8) and change in A/V ratio (V3) compared to the reference variant (V1). The choice of V1, V3, V6 and V8 could unfortunately not be made solely based on the CFD results, but also on the availability of samples.

## 4 Engine Test-Bench

The CFD investigations were able to give an insight into the mixture preparation within the pre-chamber and enables the evaluation of the conditions at ignition timing. The question that arises from those simulations is: Is a ranking based on the CFD results with respect to EGR, tke and lambda within the pre-chamber at ignition timing matching the ranking that results from test-bench measurements? A standard spark plug (SP) was used for the reference measurements, thus all pre-chamber variants are compared to it.

The operation points, which were used for the engine test-bench measurements can be found in Table 2. Compared to the CFD simulations at the test-bench operation point OP1 was adapted slightly. The difference in engine speed and load was expected to be negligible. To understand the basic effects of changing from the standard to pre-chamber spark plug lambda, SOI, FHR50% position and ignition timing were varied for OP1 and OP2 with engine parameters kept constant. The valve timings were chosen based on preliminary investigations for homogenous lean combustion operation.

Table 2: Engine operation points

Operation Points	Engine Speed [rpm]	Imep [bar]	SOI1 [°CA b. ITDC]
OP1	1250	2.7	330
OP2	2000	8	330

#### 4.1 Engine & Test Bench Setup

Investigations were performed on a multi-cylinder engine. The engine is equipped with direct fuel injection in central mounted position, which is preferable to analyze the effect of injection strategies on the pre-chamber ignition operation. To analyze combustion and gas exchange the engine is equipped with high pressure indication in the main chamber and low pressure indication within intake and exhaust ports. A high-energy ignition coil was applied on the engine. A more detailed overview on the engine and test-bench setup can be found in *Table 3*.

Table 3: Engine &amp; test-bench data

Layout	2.0 L, inline four cylinder, turbo charged
Fuel injection	DI, central mount, MHI, solenoid @ 35 MPa
Compression ratio	9.8 (without pre-chamber)
Ignition Energy	~ 140 mJ
Oil & Coolant Temperature	90 °C
Fuel	RON 95

#### 4.2 Results

Measurements were performed keeping all engine parameters constant at each operation point for each spark plug, like it was done in the CFD simulations. For all variants and the conventional spark plug lambda, SOI and FHR50 was varied. Under lean operation conditions in general the combustion is deteriorated, because additional to the residual gas the excess air increases the fraction of inert gas within the total mixture. This has an influence on both, a stable flame kernel development and the combustion speed. To investigate and evaluate whether or not the chosen passive pre-chamber spark plugs can enhance combustion and outperform the conventional spark plug will be part of the following section.

##### 4.2.1 Lambda, SOI and FHR50% Variation

In *Figure 15* measurements at OP1 are illustrated. These measurements represent results at FHR50% = 6 ° position for the lambda and SOI variation. Injection timing for lambda and FHR50% variation was set to SOI = 330 °CA bITDC position

As can be seen, stable engine operation with pre-chamber spark plug variants is only possible within a very narrow lambda range, indicating no advantage over the conventional spark plug. Even though the chosen engine roughness limit for comparing lean limit performance was put to  $CoV \leq 3\%$ , measurements above the CoV limit are also illustrated, when engine operation was possible. With the pre-chamber variants lean limit decreases by  $\Delta\lambda$  of 0.3 compared to the SP.

Higher combustion stability of the SP is also indicated by later ignition timing which alludes to a faster combustion (mainly FHR00-10% phase). All spark plugs show comparable fuel consumption at  $\lambda = 1$  the isfc (indicated specific fuel consumption).

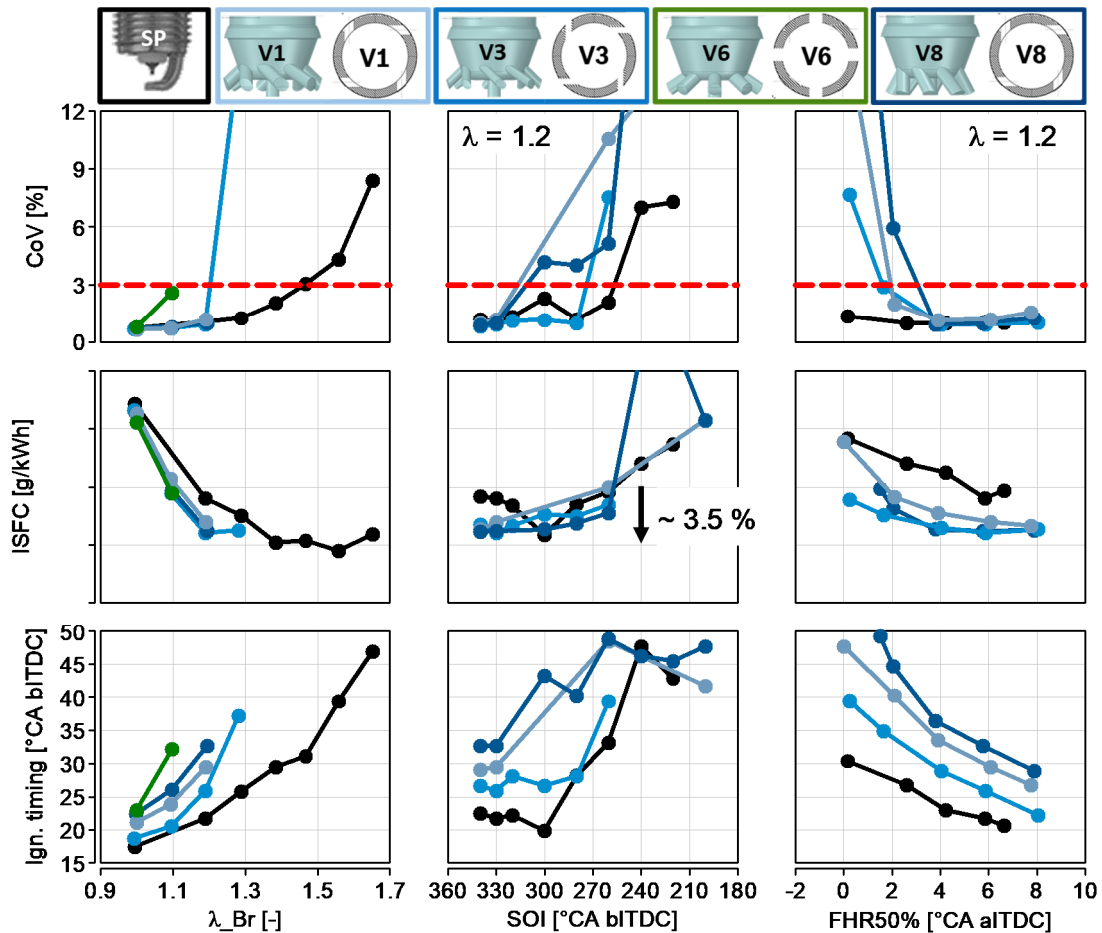


Figure 15: Comparison SP to pre-chamber, Lambda, SOI, FHR50 variation for OP1

However, under lean conditions an isfc advantage of the pre-chamber variants over the SP can be observed. The isfc advantage of the pre-chamber variants over the pre-chamber might indicate a correlation with the aforementioned lower combustion speeds. But this is not consistent, because V1 with slower combustion than V3 has higher isfc, though.

Anyway, the reason for the isfc advantage of the pre-chamber might be related to lower wall heat losses due to lower temperatures as a results of slower combustion especially in the first stage of combustion (FHR00-10%). Longer FHR00-10% durations on the other hand will lead to an increase of efficiency loss due to overall burn duration ( $dQ/d\Phi$ ).

The variant V6 shows the poorest overall performance. This is a very distinctive result, because this variant is amongst the top scoring variants shown in the CFD ranking plots shown in Figure 14. This already shows that the ranking which bases only on the ignition condition within the pre-chamber volume (EGR,  $t_{ke}$ ,  $\lambda$ ) is not always sufficient to predict the performance of a pre-chamber spark plug.

Variations of SOI and FHR50% are illustrated at a  $\lambda = 1.2$ , at which most of the pre-chamber variants are performing stable combustion.

The SOI variation shows that the pre-chamber variants are generally more sensitive with respect to the timing of the mixture preparation. The choice of SOI = 330 ° CA

bitDC proofs to be within the optimal range for the pre-chamber variants as well as for the conventional spark plug (SP). Comparing the pre-chamber variants among each other it can be stated, that the pre-chamber variant V3 shows both, a good lean limit, high robustness with SOI variation and high combustion speeds. No significant difference between the spark plugs behavior with respect to optimal combustion phasing could be observed.

In Figure 16 results at OP2 are illustrated, with  $FHR_{50\%} = 6^\circ$  and  $SOI = 330$  bitDC. Due to the higher load point all spark plugs show better lean limit performance or respectively higher combustion stability. Similarly as for OP1 the conventional spark plug is superior to the pre-chamber variants tested. The maximum achievable lambda difference between the conventional spark plug and pre-chamber is decreased from  $\Delta\lambda = 0.3$  for OP1 to  $\Delta\lambda = 0.2$  for OP2.

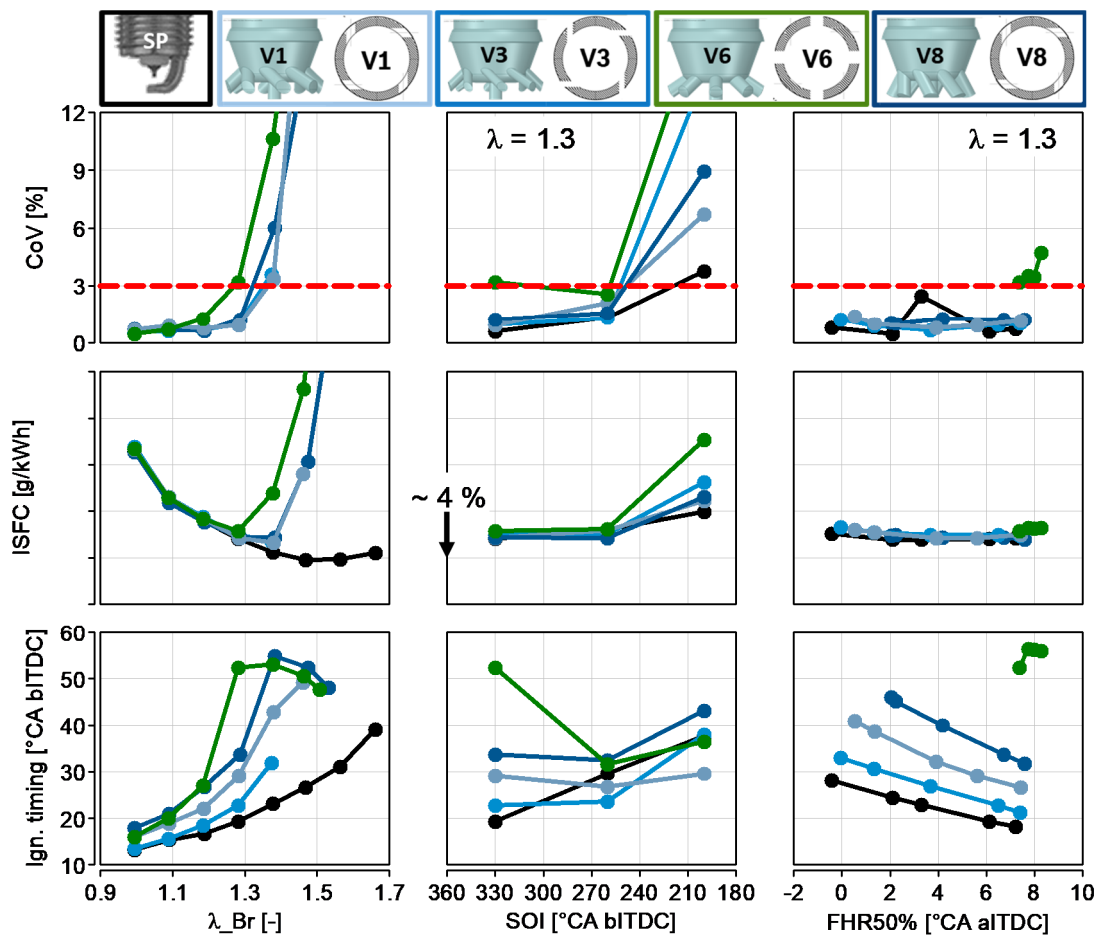


Figure 16: Comparison SP to pre-chamber, Lambda, SOI, FHR50 variation for OP2

The higher loads increase combustion stability within the main chamber in general due a higher volume specific chemically bound energy density of the mixture, higher temperatures and higher charge motion and therefor higher  $\tau_{ke}$  and better homogenization of the mixture at ignition relevant timings. This is valid for both, the pre-chamber spark-plug and the conventional spark plug. Therefor this will lead to a shorter overall combustion duration. With around a maximum fraction of 1% of total fuel captured in the pre-chamber at ITDC, the improved condition of the main chamber is therefor, leading to a decrease in  $FHR_{0-10}$  and  $FHR_{10-90}$  for both spark plug systems.

In consequence, this enables the conventional spark plug as well as the pre-chamber spark plugs to ignite at a later timing to achieve the same FHR50% position as for low loads. This, on the other hand, gives more time for the process of filling the pre-chamber with a richer gas mixture. For low loads overall combustion conditions deteriorate, therefore the pre-chamber must ignite earlier, as well as the conventional spark plug. However, if measures cannot be taken the passive pre-chamber will always have a leaner mixture. This leads to even longer combustion duration which leads to even earlier ignition timings, with even higher lambda. This process is amplified towards lower loads resulting in longer combustion durations and combustion instabilities. For example, in the above figure at  $\lambda = 1.3$  the ignition timing for variant V1 is at 30 °CA bITDC while ignition timing for SP is around 19 °CA bITDC to achieve the same FHR50%. The CFD for this operation point at 30 °CA bITDC predicts a lambda of around 1.8. Another good example of this phenomenon is the variant V6, which achieves poorest combustion stability. The variant cannot be operated at a combustion phasing earlier than FHR50% = 8 °CA aITDC for  $\lambda = 1.3$  at OP2. The other variants show a higher stability towards earlier ignition at OP2 than at OP1 (*Figure 15*). Early SOI timings show the advantage of combustion speed for the SP, while at later SOI V1 and V3 show slightly later ignition timings.

#### 4.2.2 Comparison of Rankings

At this point the engine results are compared to the CFD results with respect to ranking among the pre-chamber variants. In fact, the ranking found at the engine-test bench differs partially significantly from that made based on the CFD results. This comparison is shown in Table 4. The test-bench ranking is based on lean limit level, CoV and combustion speed. The worst performing pre-chamber variant for both, OP1 and OP2 on the engine test-bench was found to be V6, which is, especially at OP2 the second best in the CFD ranking.

Table 4: Comparison of Rankings

Operation Points	OP1 (1500/3i or 1250/3i)	OP2 (2000/8i)
CFD Ranking	V3, V8, V6, V1	V3, V6, V1, V8
Test-Bench Ranking	V3, V1, V8, V6	V3, V1, V8, V6

Furthermore, V1 shows acceptable matching at high load and rather bad matching at low load.

These results indicate, that differences among the pre-chamber variants with respect to residual gas mass fraction levels based on the CFD results are not having a significant impact on the combustion. This is clearly shown by the fact that variant V3, which has the highest residual gas mass fraction compared to the other three variants, is the best performing pre-chamber spark plug for both operation points.

Based on this comparison it becomes clear only using EGR,  $t_{ke}$  and lambda values to compare pre-chamber variants among each other is not sufficient. It shows that the quality of the combustion phase cannot be predicted solely by the mixture formation-only simulation.

## 5 3D-CFD Combustion Simulation

A 3D-CFD simulation with a focus on charge motion and mixture formation has been carried out. Based on the simulation results four samples were manufactured, which

were then tested on the test bench described above. The results is, that the CFD-simulation-based performance ranking of the different spark plugs variants does not coincide with that from the test bench. Thus with a subsequent CFD combustion simulation, the previous ranking is to be verified.

For this purpose, the calculation models of the engine including boundary conditions from chapter 3 are used. In particular constant adiabatic wall temperatures, pressure boundary conditions at the inlet and outlet ports as well as the spray conditions for gasoline injection from chapter 3 were assumed.

For a better comparability with the experimental results, the lambda and the ignition timing (Table 5) for the individual variants are used for the 3D CFD combustion simulation.

*Table 5: Lambda and Start of ignition at OP 1 and OP 2*

Variant	Variant 1 @OP1	Variant 3 @OP1	Variant 6 @OP1	Variant 8 @OP1
Lambda	1,3	1,3	1,1	1,3
Start of ignition [° CA]	673	680	669	678
Variant	Variant 1 @OP2	Variant 3 @OP2	Variant 6 @OP2	Variant 8 @OP2
Lambda	1,5	1,5	1,3	1,5
Start of ignition [° CA]	680	684	675	671

## 5.1 Validation with Testing

The combustion simulation starts when the exhaust port is open and stops shortly before the exhaust port opens again after combustion. EZFM 3-Z is used as combustion model and the turbulence model  $k-\zeta-f$  being an enhancement of the RANS  $k-\epsilon$  model, is applied.

The low load point at 1500 rpm and 3 bar indicated mean effective pressure (IMEP) (OP1) is calculated, as well as the load point at 2000 rpm and 8 bar IMEP (OP2).

### 5.1.1 Validation at OP 1

Figure 17 shows the pressure curve of the individual variants calculated with CFD (solid lines) in comparison to the test bench results (dotted lines). The black and grey colors represent the pressure of variant 1 on the test bench. Here the maximum, the minimum and the average pressure curves are shown. The pressure difference between measured maximum and minimum peak pressure is around 12 bar.

### 3.3 Combustion Systems with Direct Injection

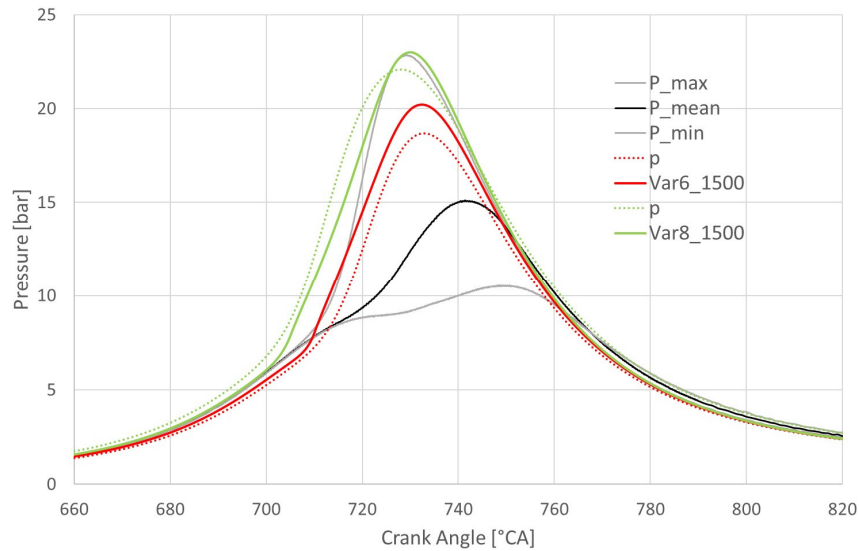


Figure 17: Comparison of CFD Results with OP 1 at test bench

Thereby a good agreement of the averaged pressure curves from simulation and measurement can be observed. The aim of the validation is to show that it is possible to achieve comparable results with the same boundary conditions and results like lambda and ignition time from the test bench. For this purpose, the combustion parameters were modified. The validation at the operating point OP 1 has succeeded very well, since the combustion parameters remained identical in the variants of the same lambda.

#### 5.1.2 Validation at OP 2

Figure 18 shows the validation at the operating point OP 2. Again, the maximum, minimum and average pressure curves of variant 1 is shown. At this Operating point the variance of pressure between maximum and minimum is lower than at OP 1. It is worth noting that all variants match the test bench results very well. Only the variant 3 exhibits a slightly larger deviation. For this deviation an in-depth explanation is given in the section 5.2.2. All variants with the same lambda can be run with the same combustion parameters.

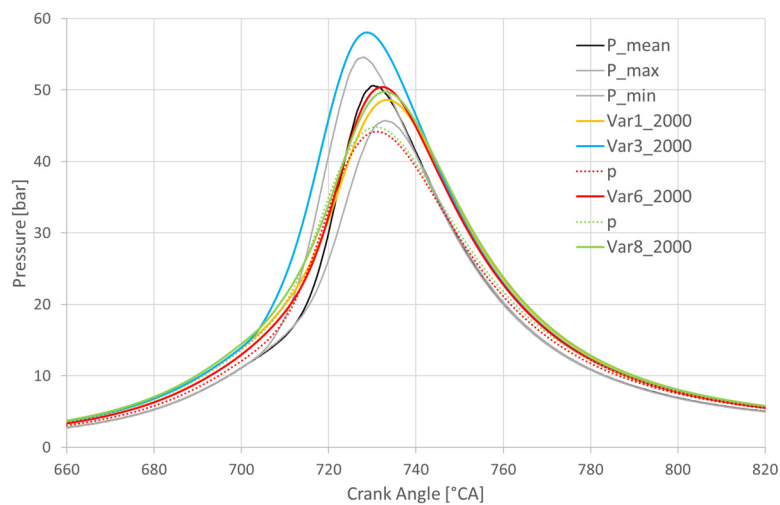
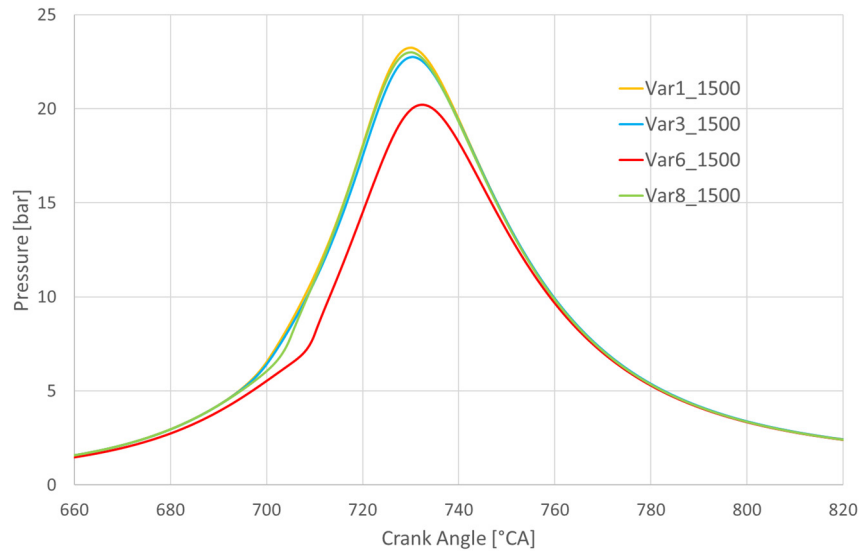


Figure 18: Comparison of CFD results with OP 2 at test bench

## 5.2 Combustion Simulation results

### 5.2.1 OP 1



*Figure 19: Peak pressure all variants at OP 1*

Figure 19 shows the pressure curve of the 4 variants at 1500 rpm at 3 bar IMEP (OP 1). It can be clearly seen that the variant 6 deviates strongly from the other variants. Table 5 shows that it is not possible for the variant 6 to perform at the comparable level with the remaining variants at this operating point with the same lambda, even at much earlier ignition times.

When, as described in chapter 3, the flow in the pre-chamber is analyzed, it can be seen that the flow direction in variant 6 is opposite to the direction of the combustion chamber (Figure 21) at the time of ignition. In variant 1, instead the flow is guided upwards on the inner wall by the tangential bores and, at ignition, the flow direction is pointing from the middle of the pre-chamber towards the combustion chamber (Figure 20).

This is the reason why the combustion predominantly moves into this direction. Figure 20 and Figure 21 show the flame front (Fluctuation Intensity) as it behaves as combustion progresses. The three related images are each taken at a distance of 1 ° CA and start with the left picture shortly after the ignition. In Figure 20 it can be seen over time that the flame front moves within 2 ° KW clearly towards the combustion chamber.

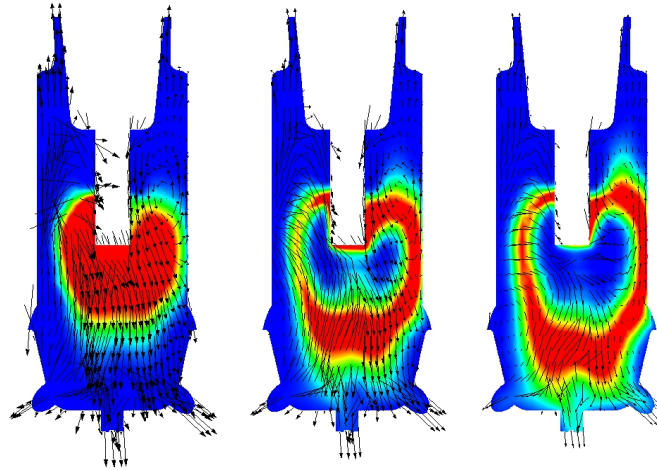


Figure 20: Fluctuation Intensity and velocity vector from Variant 1

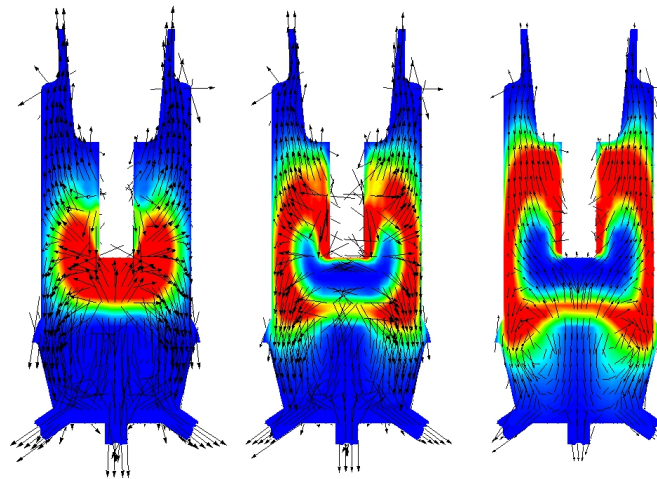


Figure 21: Fluctuation Intensity and velocity vector from Variant 6

In variant 6 (Figure 21) the flame front moves in the opposite direction during the same period ( $2^\circ$  CA) of time. This flow behavior is graphically underplayed by the velocity vectors. Figure 22 shows the lambda distribution of variants 1 and 6 including the velocity vectors. Please note, that the averaged lambda values of 1.1 and 1.3 are set for the calculation of variant 6 and variant 1 at OP 1, respectively (see Table 5). Consequently, even in variant 1, a significantly higher lambda can be seen in the upper part of the pre-chamber spark plug. But this is not critical for this variant as the combustion moves into the non-lean mixture. Variant 6 shows in Figure 22 a significantly lower peak pressure curve and therefore a much slower combustion even though it has a lower lambda and an earlier ignition timing (see Table 5). It can be seen from the right-hand image of Figure 22 that the combustion moves in the direction of a lean mixture and is therefore also significantly slowed down. Therefore, it is also understandable that this variant cannot perform well with the same lambda at the operating points OP 1 and OP 2 as the other variants.

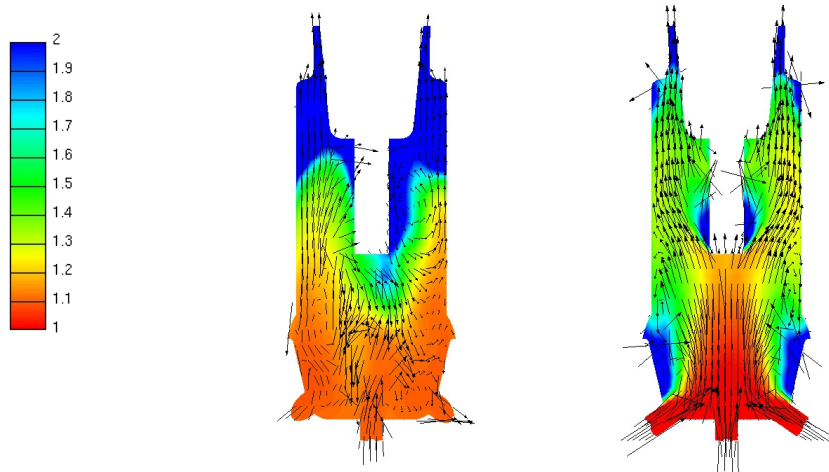


Figure 22: Lambda distribution Variant 1 and Variant 6

#### 5.2.2 OP 2

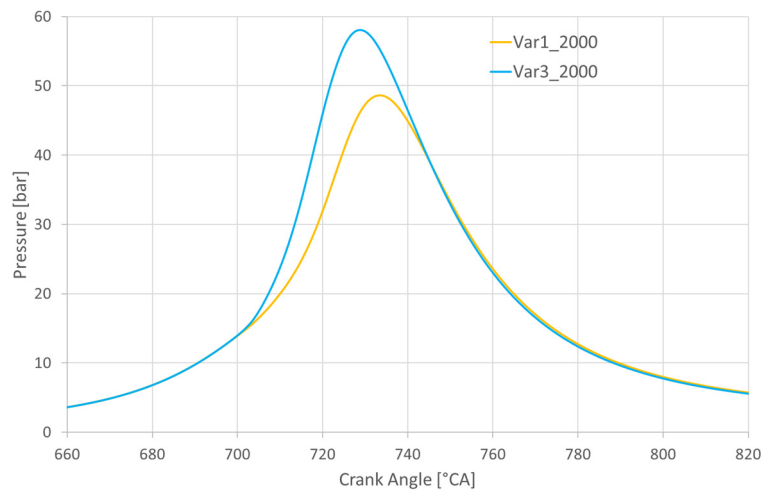


Figure 23: Peak Pressure of Variant 1 and 3 at OP 2

At operating point 2000 rpm and 8 bar IMEP, the variant 3 compared to variant 1 obviously has a much higher peak pressure and an earlier MFB50 (Figure 23). Despite the same lambda and even later ignition (about 5 ° CA) the variant 3 shows the much faster combustion. Compared to the operating point OP 1 (Figure 24) variant 1 seems to burn slightly faster. Therefore, it is quite surprising how strong the difference in the operating point with the higher load between these variants becomes. Both variants have the same geometric design of the pre-chamber spark plug. Both variants have the same number of holes and both have the same structure i.e. 8 tangential and one central hole. The only difference between these two variants is the diameter of the holes and thus the ratio of pre-chamber volume to the sum all holes' cross sections ( $V/A$ ). By changing this ratio, the pressure in the pre-chamber increases significantly to the pressure values in the main combustion chamber during combustion (Figure 25).

### 3.3 Combustion Systems with Direct Injection

This significant increase of the pre-chamber pressure causes a faster flame propagation in and a deeper flame penetration of the main combustion chamber and thus results in a significantly faster combustion in the main chamber.

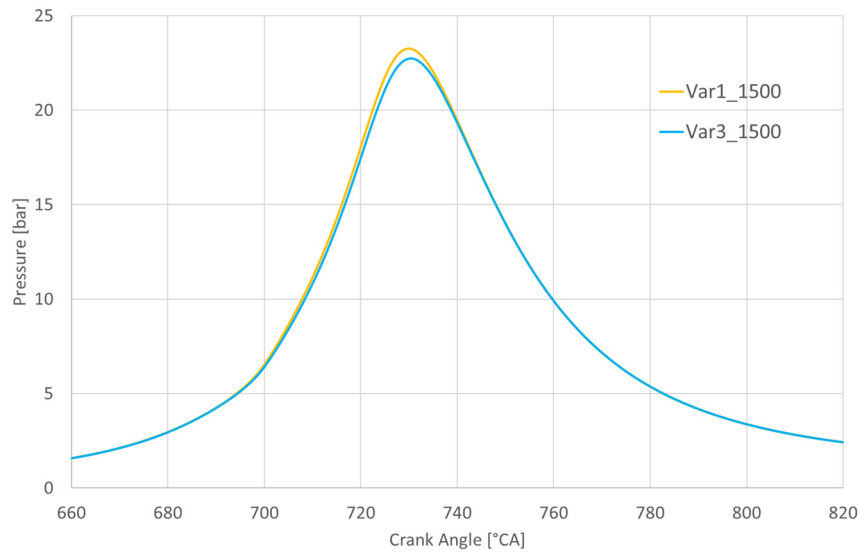


Figure 24: Peak Pressure of Variant 1 and 3 at OP 1

One observes that the penetration length of the torch of the variant 3 is much longer than from Variant 1. At the operating point OP 1, this difference is significantly less which is reflected in the nearly coinciding pressure curve (Figure 24). However, since variant 3 is ignited 7 ° CA later a faster combustion process has to be related with this variant.

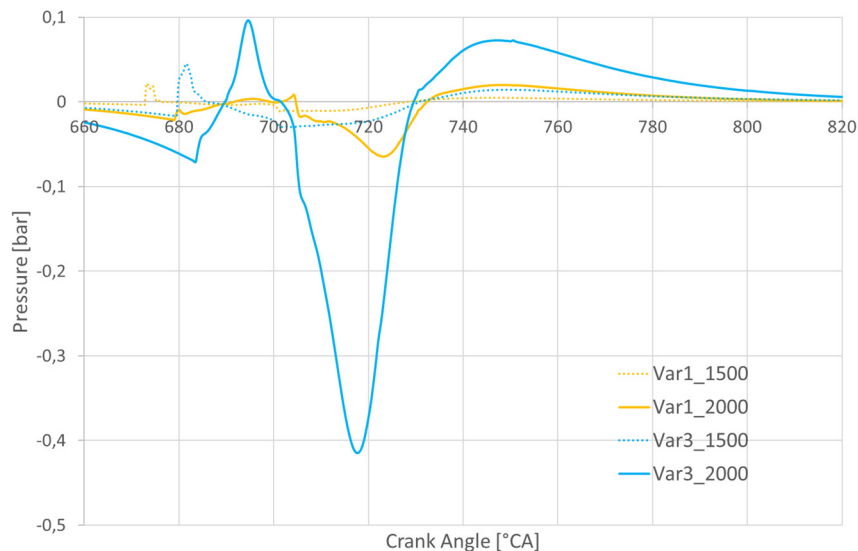


Figure 25: Pressure difference between pre-chamber spark plug and main chamber

### 5.3 Comparison of all results

For the OP1 the results can be rated by means of Figure 19. Variant 6 is easy to define on last place but all other variants are very close together. Table 5 shows the difference

in Ignition timing and therefor variant 3 is the best because of the latest time. Between variant 8 and 1 the pressure is slightly higher for variant 1, but on the other hand variant 8 will be ignited  $5^\circ$  CA later. So the ranking of OP 1 is listed in Table 6.

At OP 2 (Figure 18) the ranking for variant 3 is because of the very fast combustion and the latest time of ignition easy to define. All other variants are very similar in peak pressure. For variant 6 because of the weakness of ignite higher lambda it is obviously to rank variant 6 on the last place. The ranking for variant 1 and 8 results from the ignition timing. Table 5 shows that variant 1 can be ignited  $9^\circ$  CA later as variant 8, therefor the ranking is defines as shown in the Table 6.

*Table 6: Ranking of the Variants*

Operation Points	OP1 (1500/3i)	OP2 (2000/8i)
CFD Ranking	V3, V8, V6, V1	V3, V6, V1, V8
Test-Bench Ranking	V3, V1, V8, V6	V3, V1, V8, V6
CFD Combustion Ranking	V3, V8, V1, V6	V3, V1, V8, V6

## 6 Summary and Outlook

To evaluate the potential of the passive pre-chamber under homogeneous lean conditions, various pre-chamber spark plug geometries were designed on basis of a reference geometry. These geometries were then implemented into a 3D CFD in-cylinder model. The influence of the geometrical parameters of the pre-chamber spark plug on scavenging, turbulence generation and air-fuel mixture supply in the pre-chamber volume at two operation points were investigated. The chosen operation points contain of a low engine speed low load operation point (OP1) and one operation point at high part-load at mid-range engine speed (OP2).

To compare the pre-chamber variants amongst each other for both operation points EGR,  $\tau_{ke}$  and equivalence ratio were integrated and averaged within the pre-chamber volume at  $25^\circ$ CA before ignition top dead center (bITDC) to represent ignition conditions. Based on these values correlations among EGR,  $\tau_{ke}$  and lambda on the hand and the A/V ratios of the pre-chamber geometries to EGR,  $\tau_{ke}$  and lambda on the other hand were examined and explained. Hereafter, a ranking based on those CFD results including different weighting scenarios using EGR,  $\tau_{ke}$  and equivalence ratio values was derived. Four variants were chosen to be evaluated on the test-bench on a multi-cylinder engine against a conventional spark plug.

For OP1 and OP2 and an engine roughness limit of  $CoV \leq 3\%$  the highest lambda is achieved with the conventional spark plug. However, at the low load operation point (OP1) under lean conditions the passive pre-chamber spark plug variants show a fuel consumption advantage over the conventional spark plug. At isfc optimal engine operation the combustion speeds of the pre-chamber variants are lower than for the conventional spark plug.

On basis of these engine test-bench results a ranking was derived based on the performances of the pre-chamber using engine roughness/stability and maximum achievable lean limit as criteria.

The comparison between the CFD rankings which so far were solely made based on evaluating the condition in the pre-chamber at ignition timing (without combustion) and the engine test-bench ranking of the pre-chamber variants displayed significant discrepancies. To understand this divergence 3D-CFD combustion simulations were conducted additionally to the aforementioned simulations of gas exchange and mixture preparation.

In order to verify the results of the test bench or the differences between the two results, the 3D-CFD combustion simulation was performed. The combustion simulation was validated with the measurement results. The same combustion parameters were used for the different variants with respect to the same operating points as long as they had the same lambda. Variant 6 deviated significantly from the other variants. This difference could also be explained on the basis of the combustion results, furthermore the difference between variants 1 and 3 is clarified with the A/V ratio.

The influence of the ratio of area to volume (A/V) is decisive for the combustion result. As a result of the combustion simulation a new ranking for the pre-chamber variants was made. This new ranking matched better to the ranking from the engine test-bench than the original CFD ranking which was derived from simulations without combustion considered.

Due to the fact that hardware test and investigations are expensive 3D-CFD combustion simulation is an attractive alternative to develop pre-chamber spark plugs.

In fact, this study showed that for CFD support of pre-chamber spark plug design development combustion simulation is necessary.

## Literatur

- [1] M. Blankmeister, W. Niessner, M. Günther, R. Tröger, C. Grünig, Optimization of Passive Chamber Spark Plugs to Improve Lean Mixture Operation in Gas Engines, 2<sup>nd</sup> International Conference on Ignition Systems for Gasoline Engines 2014
- [2] W. Niessner, A. Schenk, A. Ernst, U. Sander, Zündkerze für eine mit Gas betriebene Brennkraftmaschine, 2009 Patent DE 102010004851 B4
- [3] C. Heinz, S. Kammerstätter, T. Sattelmayer, Vorkammerzündkonzepte für stationär betriebene Großgasmotoren, MTZ - Motortechnische Zeitschrift Issue 1/2012
- [4] S. Biswas, S. Tanvir, H. Wang, L. Qiao, On ignition mechanisms of premixed CH<sub>4</sub>/air and H<sub>2</sub>/air using a hot turbulent jet generated by pre-chamber combustion, Applied Thermal Engineering 106 (2016) 925–937